

AD-A077 377

CATHOLIC UNIV OF AMERICA WASHINGTON D C DEPT OF PHYSICS F/G 20/13
THEORY OF SUPERCOOLED LIQUIDS; PHASE DIAGRAM OF WATER; PRIENTAT--ETC(U)
DEC 70 P H MEIJER N00014-78-C-0518

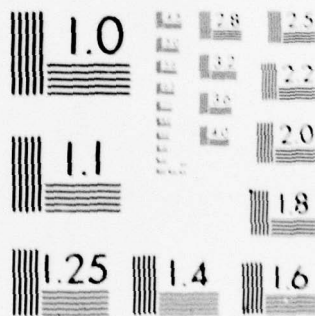
UNCLASSIFIED TR-1

NL

1 OF 1

AD
A077377





MICROCOPY RESOLUTION TEST CHART
NATIONAL BUREAU OF STANDARDS-1963-A

AD A 077377

DDC FILE COPY

OFFICE OF NAVAL RESEARCH
Contract N00014-78-C-0518
Task No.
TECHNICAL REPORT NO. 1

(12)

LEVEL II

DDC
RECEIVED
NOV 28 1979
RECEIVED
A

The Catholic University of America
Department of Physics
Washington, DC 20064

November 1979

Reproduction in whole or in part is permitted for
any purpose of the United States Government

This document has been approved for public release
and sale; its distribution is unlimited

79 11 28 044

REPORT DOCUMENTATION PAGE		READ INSTRUCTIONS BEFORE COMPLETING FORM
1. REPORT NUMBER Report Number 1	2. GOVT ACCESSION NO. (10)	3. RECIPIENT'S CATALOG NUMBER Paul H. E. MEIJER
4. TITLE (and Subtitle) (6) Theory of Supercooled Liquids; Phase diagram of water; Orientational dependent interactions.		5. TYPE OF REPORT & PERIOD COVERED (9) Technical Report
7. AUTHOR(s)		6. PERFORMING ORG. REPORT NUMBER --
9. PERFORMING ORGANIZATION NAME AND ADDRESS Catholic University Physics Department Washington, D.C. 20016		8. CONTRACT OR GRANT NUMBER(s) (15) N00014-78-C-0518
11. CONTROLLING OFFICE NAME AND ADDRESS Office of Naval Research Arlington, VA 22217		10. PROGRAM ELEMENT, PROJECT, TASK AREA & WORK UNIT NUMBERS (12) 52
14. MONITORING AGENCY NAME & ADDRESS (if different from Controlling Office) (14) TR-1		12. REPORT DATE (12) Dec 1970
		13. NUMBER OF PAGES 17 + 29 = 46
		15. SECURITY CLASS. (of this report) Unclassified
		15a. DECLASSIFICATION/DOWNGRADING SCHEDULE
16. DISTRIBUTION STATEMENT (of this Report) This document has been approved for public release and sale; its distribution is unlimited.		
17. DISTRIBUTION STATEMENT (of the abstract entered in Block 20, if different from Report)		
18. SUPPLEMENTARY NOTES Section II, "Lattice model of water", will be submitted for publications		
19. KEY WORDS (Continue on reverse side if necessary and identify by block number) Water, equation of state, phase diagram of supercooled state, hydrogen bond, maximum density. Instability in BBGKY-formalism. Orientation dependent forces. Phase diagram of anti-ferro magnetic systems.		
20. ABSTRACT (Continue on reverse side if necessary and identify by block number) Part 1: We investigated the question whether one can conclude from BBGKY theories whether instabilities do occur in a liquid at low temperatures. Several authors denied this possibility and we show that such results are due to the assumptions they made. → next page		

Part 2: In order to calculate the phase diagram of water we introduce a lattice model that has the following features. A nearest neighbor attraction, which is strongly dependent on the relative orientation of water molecules, due to hydrogen bonding and a next nearest neighbor or three body repulsion. The hydrogen bonding is introduced with the help of a set of weight factors in accordance with Pauling's ice rules. The entropy is calculated according to the cluster variation method for tetrahedrons. The isotherms show a maximum in the density and a phase separation between the vapor, the open ice state and a state which is dense packed.

Part 3: To see how orientational dependent forces influence the supercooling process, the simplest model known (Barker and Fock model) is analysed. It is shown under what conditions the phase diagram becomes topologically different from the simple Ising phase diagram.

Part 4: Preparatory work for the determination of the characteristic points in the phase diagram of an antiferromagnet.

Accession For	
NTIS GADR	<input checked="" type="checkbox"/>
DLG TAB	
Unannounced	
Justification	
By	
Distribution	
Availability Codes	
Dis	Avail and/or special
A	

This report consists of four parts:

1. Possible instabilities in the liquid structure leading towards the formation of a solid (work with Y. M. Wong).
2. Calculation of a water model with the clustervariation method. Phase diagram and undercooling features.
3. Influence of orientation on the undercooling process (work with E. Bodegom).
4. Transition points in antiferromagnetic systems (work with S. Eckmecki).

I. Instabilities in the distribution function for a dense system.

1. Introduction.

We are addressing ourselves to the question of whether and how the distribution function of a dense system becomes unstable upon lowering the temperature. As is evident from the observation: a solid is formed. Just lowering the temperature does not create a solid however, it creates a metastable situation. Does this metastable situation finally become unstable at a still lower temperature?

Originally Kirkwood¹ pointed out that this is the case, but in several subsequent papers it was pointed out first by Kunkin and Frisch,² later by Nagai and Naitoh³ and also by Muller-Krumbhaar and Haus⁴ that the instability predicted by the linearized theory disappeared when one goes to higher approximations.

This note is to point out that this conclusion is not necessarily true for the general case in which no successive approximations are introduced. Since it is impossible to calculate the general case completely we will have to rely on another, but far more sensible, approximation. This approximation was proposed by Kozak, Weeks and Rice⁵ and uses the observed fact that the density of the liquid and the density of the solid differ very little. We re-analyzed the situation and found that there is no contradiction between the general liquid theory and the occurrence of an instability in this

medium; whether such instability leads to a period structure is an open question.

2. The BBGKY-formalism.

The starting equation is the lowest member of the BBGKY hierarchy. It is given by

$$-\frac{\partial}{\partial R_1} \ln \varrho(R_1) = \beta \int \frac{\partial U(R_{12})}{\partial R_1} \varrho(R_2) g^{(u)}(R_{12}) dR_2 \quad (1)$$

(See for instance Balescu⁶) where $\varrho(R_1)$ is the singlet density, $u(R_{12})$ the pair potential and $g(R_{12})$ the pair correlation function. The integral is over the volume and β represents the temperature. Following Hiroike⁷ we find from eq.(1)

$$\ln c \varrho(R_1) = \beta \int_V dR_2 \varrho(R_2) \int_{R_{12}}^{\infty} dr u(r) g^{(u)}(r) \quad (2)$$

where $c = c(\varrho)$ is a constant in space depending on the average density ϱ . This expression can be written in the Hammerstein⁸ form, if one puts:

$$\phi(1) = \ln c \varrho(1) \quad (3a)$$

and

$$K(12) \equiv \frac{\beta}{c} \int dr u'(r) g^{(2)}(r) \quad (3b)$$

giving

$$\phi(1) + \int K(12) \exp(\phi(2)) d2 = 0 \quad (4)$$

Next we follow the non-linear equation approach of Week, Rice and

Kozak⁵ in which we search for two solutions ϕ_1 and ϕ_0 differing little in density. We define

$$\gamma(1) \equiv \phi_1(1) - \phi_0(1) \quad (5)$$

where ϕ_0 refers to the liquid and ϕ_1 to the new solution. The solution ϕ_1 satisfies equation (4) with

$$K(12) = K(|1 - 2|),$$

but for ϕ_1 no such assumption will be made. This is important since this type of equality definitely does not hold for a solid. In fact, any such assumption made on the second solution prevents the solution of corresponding to a solid.

Substituting (5) into (4) gives

$$\gamma(1) + \int L(12)(e^{\gamma} - 1) \quad (6a)$$

with

$$L(12) \equiv K(12)\exp \phi_0(2) \quad (6b)$$

Making use of the fact that the density of the new phase differs very little from that of the fluid phase, we can expand the exponent in the Kernel, whereupon we obtain the linear integral equation:

$$\gamma(1) + \int L(12)\gamma(2)d2 \quad (7)$$

which can be solved by a Fourier transform in space

$$\gamma(k)[1 + L(k)] = 0 \quad (8)$$

For the existence of a non-trivial $\gamma(k)$, one requires therefore

$$1 + L(k) = 0 \quad (9)$$

i.e. in three dimensions one requires

$$1 + \frac{4\pi}{k} \int L(R)R \sin(kR) dR \quad (10)$$

Following Kunkin and Fritsch² we will apply this to the hard core system. This is not a very good system since it does not give

rise to a solid in the ordinary sense of the word. We write out this example to show that one obtains the same result in this case, but without the more stringent assumptions that they used.

3. Hard sphere system.

For hard spheres, one has

$$\frac{du}{dr} = -\frac{1}{\beta} \delta(r-d_0) \quad (11)$$

where d_0 is the diameter of the hard sphere. Inserting this in (10) gives

$$1 + \frac{4\pi}{k} \int_0^{d_0} \rho g(d_0) R \sin kR = 0 \quad (12)$$

which does not depend on the temperature, as it should not. This can be rewritten as

$$1 + \frac{4\pi d_0^3}{z^3} \rho g(d_0) [\sin z - z \cos z] = 0 \quad (13)$$

with $z = kd_0$. We used the following expression for the Kernel

$$L(R) = g^{(2)}(d_0) \theta(d_0 - R)$$

4. Discussion

The expression (13) is exactly the expression that was used by Kirkwood, except that no inconsistent (and unjustified) linearisation is used on the $\rho(R_1)$ and the $g(R_{12})$, contrary to Kunkin and Frisch² and Naitoh and Nagai.³ The only assumption is the step from (6) to (7), which is plausible in the sense that it is in step with the observation.

The occurrence of a second solution, also called branching or bifurcation, does not imply crystallization, i.e. a periodic solution. This is certainly not the case for hard spheres, where van Hove proved⁶, in one dimension, that no periodic solution exists. For the non-hardsphere case the question is left open. There exists some work by Ventevogel and Nyboer⁹ on the spontaneous occurrence of periodic structures at zero temperatures.

Other approaches¹⁰ using the exact solution for $C(1,2)$, the direct correlation function or $g(1,2)$, the indirect correlation functions from the Percus Yevich equation support the absence of instabilities in three dimension.. This could be due to the Percus Yevich equation, which despite its appeal is nevertheless an approximate equation.

Finally we remark that the decoupling schemem used by Muller-Krumbhaar and Haus⁴ is not well understood, that is, we do not know whether it will a priori prevent instabilities to show up.

REFERENCES

1. J. G. Kirkwood in Phase Transformations in Solids, ed. by R. Smoluchowski, J. E. Mayer and W. A. Weyl (Wiley, NY, 1951) p.67 and A. A. Vlasov, Many Particle Theory and Its Applications to Plasmas (Gordon and Breach, NY, 1961).
2. W. Kunkin and H. L. Frisch, J.Chem.Phys. 50, 1817, 1969.
3. T. Naitoh and K. Nagai, J. Stat. Phys. 11, 391, 1974.
4. H. Muller-Krumbhaar and J. W. Haus, J. of Chem. Phys. 69, 5219, 1978.
5. a) J. D. Weeks, S. A. Rice and J. J. Kozak, J. Chem. Phys. 52, 2416, 1970.
b) J. J. Kozak, S. A. Rice and J. D. Weeks, Physica (Utr.) 54, 573, 1971.
6. R. Balescu, Eq: and Non-eq: Statistical Mechanics, A. Wiley-Interscience, NY, 1975.
7. K. Hiroike (see comment in 5b).
8. A. Hammerstein, Acta. Math. 54, 117, 1930.
9. W. J. Ventevogel and B. R. A. Nijboer, preprint.
10. The indirect coupling approximation mentioned in Sec. VII of 5a.

II. Lattice model of water.

For this section of the report: see the attached preprint.

III. Orientational models

One of the most interesting cases in which orientational interaction plays a role is the phase diagrams of binary liquids that show both upper and lower critical temperatures. This phase diagram was for the first time successfully explained by Barker and Fock¹ and it was subsequently described in more detail in a series of papers by Wheeler e.a.² In this field we obtained the following results. It is possible to map the Barker and Fock model on a cluster variation type of description in a one-to-one correspondence. The advantage of this mapping is that one can easily generalize to larger clusters. Barker and Fock use only pairclusters. Second, we found that it is not necessary to tie in the number of orientations with the coordination number of the lattice and one can generalize the model accordingly.

The most important question is, however, why and when this model does give the lower critical point. This we succeeded in explaining as follows. One can make a reduction, somewhat similar to the reductions used in the Niemeijer and van Leeuwen transformations or in the theories of decorated lattices. These transformations lead to a model without orientational degree of freedom but with one or more temperature dependent coupling constants. By studying the temperature dependent coupling constants, mainly graphically, one can observe under what circumstances new critical temperatures will occur.

III. Orientational models

One of the most interesting cases in which orientational interaction plays a role is the phase diagrams of binary liquids that show both upper and lower critical temperatures. This phase diagram was for the first time successfully explained by Barker and Fock¹ and it was subsequently described in more detail in a series of papers by Wheeler e.a.² In this field we obtained the following results. It is possible to map the Barker and Fock model on a cluster variation type of description in a one-to-one correspondence. The advantage of this mapping is that one can easily generalize to larger clusters. Barker and Fock use only pairclusters. Second, we found that it is not necessary to tie in the number of orientations with the coordination number of the lattice and one can generalize the model accordingly.

The most important question is, however, why and when this model does give the lower critical point. This we succeeded in explaining as follows. One can make a reduction, somewhat similar to the reductions used in the Niemeijer and van Leeuwen transformations or in the theories of decorated lattices. These transformations lead to a model without orientational degree of freedom but with one or more temperature dependent coupling constants. By studying the temperature dependent coupling constants, mainly graphically, one can observe under what circumstances new critical temperatures will occur.

Usually undercooling can be obtained very easily in substances with "sticky" molecules. Hence we tried a simple model of such a system. The model uses a lattice gas of two types of molecules A and B on each lattice site and each molecule has γ contact points. Of these γ contact points γ_1 are "sticky" and γ_2 are not. We assume that between the A and the B molecules we have the following energy expression: if either one or both contact points of a pair of molecules are sticky they attract each other and if both are of the non-sticky kind they repel. We choose this example since Barker and Fock have shown that this case leads to a lower critical point. However, it is easy to show that this is one example out of a class of systems.

The entropy for such a system in the notation of Kikuchi is given by (we start out with the pair approximation):

$$S/N = \ln \frac{\prod_{A,B} (x_i L)!^{z-1}}{\prod (\gamma_{ij} L)! g_{ij}^{z/2} L!^{z/2-1}}$$

where L is the number of lattice points, x_A and x_B the site variables and y_{ij} the sixteen pair variables of the problem. The coordination number is z and the weight factors g_{ij} are given by:

$$g_{ij} = g_i g_j$$

and

$$g_1 = g_3 = \gamma_1 / (\gamma_1 + \gamma_2)$$

$$g_2 = g_4 = \gamma_2 / (\gamma_1 + \gamma_2)$$

the resulting free energy per site is given by

$$f = \frac{F}{N} = \frac{z}{2} \sum g_i g_j \varepsilon_{ij} \gamma_{ij} - kT \left\{ (z-1) \sum_{A,B} x_A (\ln x_A - 1) \right. \\ \left. - \frac{z}{2} \sum g_i g_j \gamma_{ij} (\ln \gamma_{ij} - 1) - \left(\frac{z}{2} - 1 \right) \right\}.$$

where z is the number of nearest neighbors.

The constraints on the pair variables are

$$x_A = \sum_j g_j \gamma_{ij} ; (\lambda_i) ; i=1,2$$

$$x_B = \sum_j g_j \gamma_{ij} ; (\lambda_i) ; i=3,4$$

with the appropriate Lagrange multipliers behind the semicolons.

With these terms inserted, we minimize the extended free energy

$$\frac{\partial}{\partial \gamma_{ij}} \left(f + kT \frac{z}{2} \left\{ \sum_i \lambda_i g_i (x_i - \sum_j g_j \gamma_{ij}) \right\} \right) = 0$$

leads to

$$\gamma_{ii} = e^{\lambda_i}, \quad \gamma_{ij} = \exp\{(\lambda_i + \lambda_j)/2\} \cdot e^{-\beta \varepsilon_{ij}}$$

since we assumed no interaction between like molecules.

The chemical potential μ_A is found from $\partial f_{\text{ext}} / \partial x_A$ which gives

$$\begin{aligned}\mu_A &= -kT(z-1) \ln x_A + \frac{z}{2} kT (g_1 \lambda_1 + g_2 \lambda_2) \\ &= -kT \left\{ (z-1) \ln x_A + \frac{z}{2} g_1 \lambda_1 + \frac{zg_2}{2} \ln \gamma_{12} \right\}\end{aligned}$$

and similar for μ_B . If the solution has two roots $(\mu_A)_1$ and $(\mu_A)_2$ we deal with coexisting phases.

To solve the system we simplify the notation. Define

$$X_i = \sqrt{g_{ii} \gamma_{ii}} \quad \text{and} \quad \eta_{ij} = e^{-\beta \epsilon_{ij}}$$

We find the following system of equations for the variables

x_1, \dots, x_4

$$X_i \sum_j X_j \eta_{ij} = g_i x_i$$

where $x_1 = x_2 = x_A$ and $x_3 = x_4 = x_B$.

REFERENCES PART III

1. J.A.Barker and W.Fock, Discussions Faraday Soc., 15, 188, 1953.
2. G.R. Anderson and J.C. Wheeler, J. Chem Phys. 69, 2082 and 3403, 1978.

IV. Antiferromagnetic transition points.

We address ourselves to the question of the transition points of a mixed antiferro and ferromagnetic system; a so-called metamagnet. The global phase diagram of a metamagnet consists of a Neel temperature (a transition to the antiferromagnetic state at zero field) and a line of second order transitions, a possible tri-critical point, a line of first order transitions for zero staggered field and lines of first order transitions in non-zero staggered fields. These options were described by Kincaid and Cohen¹ who showed how the various phases can be obtained from a Landau-Ginsburg expression in the various order parameters. If we ignore the non-analytic behavior near the critical points, this free energy is an analytic expression and they computed the various coefficients using the mean field theory. Under this assumption they find that there are two regions for the coupling constant ratio $J_F/J_{AF} = \xi$. One region $\xi > \xi^*$ leads to a tri-critical point, the other to a so-called bi-critical end (BC) point. We found 2) that the next higher approximation, the Bethe approximation, leads to a set of phase diagrams with BC points only. Despite the fact that this approximation gives generally much better results for the (absolute) critical temperature, there are reasons to believe that the Bethe approximation does not take enough detail into account. (By absolute critical temperature we mean to refer to those experiments where both the temperature and the coupling constants are known and not, as is unfortunately always almost the case, where the critical temperature is measured without any

further information about the coupling constants.) Returning to the fact that the Bethe approximation may not always give the details of the phase diagram; a most striking example is the work on the AB alloys³ where only the tetrahedron approximation started to give a complete phase diagram. Consequently we want to study the metamagnet using the cluster variation method.

The cluster variation method requires more information about the lattice than the Bethe approximation. In the latter it suffices to specify the number of nearest and next-nearest neighbors. For larger clusters we have to give the detailed information not only of the lattice, but also of the substructures we expect to obtain in the antiferromagnetic ordering. After some discussion we decided to study the following cases: 1) the bcc subdivided in two sc, 2) the sc subdivided in two fcc, and 3) the fcc in subdivided two substructures as mentioned in Li.⁴ Finally we evaluated the 2 dim. square into two 2 dim. square lattices in order to have an test case.

At this moment we have determined the free energy expressions for these four cases. In order to calculate the free energy in the cluster variation method one needs the cluster relations between the various order parameters and their weight factors in order to construct the corresponding entropy expressions. This work is being done by Mr. Servet Eckmeckl.

REFERENCES PART IV

- 1) J. M. Kincaid and E. G. D. Cohen Physics Letters 50A 317, 1974 and Physics Reports 22, 57, 1975
- 2) P. H. E. Meijer and W. C. Stamm Physica 90A, 77, 1978
- 3) R. Kikuchi, J. Chem. Physics 60, 1071, 1979 (Figure 7) and C. M. van Baal, Physica 64, 571, 1973
- 4) Y-Y. Li, Phys. Rev. 100, 627, 1955
- 5) B. Nienhuis and M. Nauenberg Phys. Rev. B 13, 2021, 1976

List of Visitors

Dr. Pierre Papon, Lab. for Thermal Physics, Ecole Supérieure
of Physics and Chemistry. University of Paris.

Dr. J. Teixeira, Lab. for Thermal Physics. Ecole Supérieure
of Physics and Chemistry. University of Paris.

Dr. A. Nihat Berker, Physics Department, Mass. Inst. of Technology.
Cambridge, Mass.

Dr. Lukas Turski, Institute of Theoretical Physics, Warsaw
University, Poland.

Dr. Alf Sjölander, Argonne Nat. Lab. Solid State Science Division,
Argonne, Illinois and Inst. of Theoretical Physics, Chalmers
University of Technology, Goteborg, Sweden

Participants

P. H. E. Meijer	Principal Investigator
Y. M. Wong	Post doc
E. V. Royen	Consultant
E. Bodegom	Grad Student
S. Eckmecki	Grad Student

Phase diagram of water based on a lattice model.

I. Introductory formulation

Paul H. E. Meijer
The Catholic University of America
Washington, DC 20064

Ryoichi Kikuchi
Hughes Research Laboratories
Malibu, CA 90265

and

Pierre Papon
Ecole de Physique et de Chimie
10 rue Vauquelin, 75231 Paris, FRANCE

ABSTRACT

In order to calculate the phase diagram of water we introduce a lattice model that has the following features. A nearest neighbor attraction, which is strongly dependent on the relative orientation of water molecules, due to hydrogen bonding and a next nearest neighbor or three body repulsion. The hydrogen bonding is introduced with the help of a set of weight factors in accordance with Pauling's ice rules. The entropy is calculated according to the cluster variation method for tetrahedrons. The isotherms show a maximum in the density and a phase separation between the vapor, the open ice state and a state which is dense packed.

Keywords: water, equation of state, cluster variation method, entropy, ice, maximum density in water, hydrogen bond.

INTRODUCTION

In two of his recent papers, Bell^{1,2} developed a lattice model in calculating the phase diagram of water. He used a bcc lattice and placed oxygen atoms and vacancies on the lattice points; hydrogen atoms in water molecules lie on body-diagonal bonds connecting nearest-neighbor lattice points.

The bcc lattice is made of two interpenetrating diamond-type sublattices, and thus we can define the ordered and disordered phases based on these two sublattices. In this way of treatment, liquid water is in a disordered state that lies between two ordered states. One ordered state is the dense bcc state, associated with ice VI, and the other state has only half of the available sites occupied (i.e. one sublattice is almost fully occupied and the other sublattice almost empty). This open structure we associate with ice I. Which of the states is formed depends of course on the pressure and the temperature. Although for the full treatment of these two phase transitions one needs a two sublattice model, in this introductory Part I we will explain the key points of the treatment without using the sublattices in order not to complicate mathematics. The sublattice treatment is presented in the accompanying Part II.³

In order to make the lattice model as water-like as possible, we build in two features, as was done by Bell.¹ The first feature is the presence of the hydrogen bond between two water molecules. The hydrogen bond has the result that two neighboring molecules have an interaction potential that depends on the relative orientation: if mutually aligned in the proper

way, there is a very strong binding force; if not mutually aligned, the force between the two water molecules is weak. If the water molecule, which has a V-shape, is placed in the body-center of a cube, the two hydrogen "arms" can be laid in 12 different ways along the eight body diagonal-halves that radiate from the body-center. It is tacitly assumed that the water molecule always prefers solely these orientations, even in the absence of neighbors. If we pick a pair of water molecules, the number of orientations will be 144, and it is easy to show that 18 of these lead to hydrogen bonding. The combinatorial calculation is in fact identical with the one made by Pauling⁴ to obtain the entropy of ice at zero degrees.

The second feature of the Bell model is the use of a repulsive three-body force. Bell reasons that this force discourages too close a packing and may be the main reason why a negative expansion coefficient in water is found. Whether an actual three-body force really exists is an open question, despite the fact that such forces are often proclaimed in the literature,⁵ because there is really no direct evidence for its presence in nature. All conclusions were based on the necessity to fit the data. The lattice models work with the same kind of handicap: except for the hydrogen bond energy, we do not have an independent and consistent estimate of the other coupling parameters in our model; hence we have to work backwards from the known isotherms. In this paper we restrict ourselves to work with one set of parameters, taken from a melange of information available.

Figure 1 shows the lattice structure we use in our formulation. The positions A form a diamond lattice and the positions B, which form by themselves also a diamond lattice, will complete this to a bcc lattice. In the treatment in this paper we choose a tetrahedron as indicated in Fig. 1 as the basic cluster. In this tetrahedron two of its corners are on the A sublattice and two of its remaining corners are on the B sublattice. Of the six edges, four are nearest neighbors and two are next-nearest neighbors.

The method used to obtain the expression for the free energy was developed by one of us^{6,7,8} and was successfully applied to a large variety of models. In Section 2 we will give a description, but the main idea is the following. If one writes down the entropy associated with a cluster of, say four, particles using the Boltzmann expression one has made an overcount. This overcount has to be corrected by subtracting partial entropy contribution due to clusters of smaller size. The entropy of these subclusters again contains an overcount, which has to be corrected by considering still smaller clusters, and so on.⁹ The result differs substantially from the expressions used by Bell and his co-workers. In his one-sublattice case¹ he introduces the entropy of the tetrahedrons and of the point variables, but omits all intermediate clusters. On the other hand in the two-sublattice paper Bell and Salt² use the point-variable entropy only, which reduces the model to the simplest mean field calculation.

In order to facilitate the computations we introduce a cluster relation CR-matrix, given in Appendix I. Using this CR-matrix we can write down the expression for the entropy and hence the grand-potential function Φ . Minimization of the latter leads then to the most probable, i.e. equilibrium, distribution of the largest clusters. This variation of the Φ with respect to the order parameters, ten in our case, leads to a set of self-consistent equations. Kikuchi has pointed out^{10,11} that this set of equations can be solved in a natural way. Natural meaning that the corresponding free energy is always decreasing during the iterative process. This method is used here, too, and the solutions, where obtained, are practically at the limit of the accuracy of the computer.

2. Description of the model.

In Figure 2 we give the set of ten clusters introduced by Bell as well as all the resulting subclusters. The open circles refer to the absence of a particle, the closed circles to the presence of an oxygen atom. Hydrogen atoms attached to the oxygen atom are not shown except for the H-bond cases. One connecting line represents a nearest neighbor bond, two connecting lines represent a next-nearest neighbor bond. The nearest neighbor bond is either "blank" or has an "H" (actually two crosslines) to indicate whether that particular pair of occupied sites is or is not hydrogen-bonded. Note that there are two types of pair bonds: y and z. The z-bonds are next-nearest neighbor bonds and do not depend on the relative orientation of the two water molecules at the pair, while y-pair bond refers to

nearest neighbors and has two options: with and without an H-bond, resulting in the Pauling-ratio of weight factors: one to seven. In the table we distinguish between the orientational weight factors g_o on the right, and the topological weight factors g_t on the left. The g_t is the number of different configurations when the molecules and h-bonds are moved around in the tetrahedron. The g_o is the number of ways the hydrogen atoms can be placed next to the oxygen molecules. The two weight factors, the topological and the orientational, enter the calculation in a different way. In what follows, anything that is simply called the weight factor is the product of the two: $g_i = (g_t g_o)_i$ for the i^{th} configuration.

In order to derive the cluster relations we observe that each cluster can be augmented by one more site to form the next larger cluster. Take for instance the cluster called u_1 . If this cluster is completed into a tetrahedron, the added site can be either occupied or not occupied. This leads to:

$$u_1 = w_1 + 12w_2 \quad (2.1)$$

since occupation can take place in 12 different orientational ways of the hydrogen atoms. The parameters x can be completed into a linear combination of z 's and also into a linear combination of y 's. In such cases both relations should hold. This procedure is not unambiguous. There is a bifurcation in y_2 which can be written as two different linear combinations of u 's:

$$y_2 = u_2 + 12u_4 = u_3 + \frac{21}{2}u_5 + \frac{3}{2}u_6 \quad (2.2)$$

These subclusters are defined in Figure 2. It is clear that during the construction of these relations, one should use the orientational weight factors. The normalization relations of the

w's, the u's, the z's, the y's, and the x's, use the total weight factors. The result of the calculation is given in Appendix I, in the form of a matrix where all triple, pair and single cluster parameters are written as linear combinations of the tetrahedral cluster parameters, w_i ($i = 1, \dots, 10$). In Table I the y_2 expression, for example, satisfies both the right-hand u sums (2.2). We now introduce the our model.

3. Determination of the entropy.

The entropy for the tetrahedral model on a bodycentered cubic lattice can be written symbolically as⁶:

$$S = k_B \ln \left\{ \frac{\left\{ k \begin{smallmatrix} i \\ \parallel \\ j \end{smallmatrix} \right\}_N^{12} \{l\}_N}{\left\{ k \begin{smallmatrix} i \\ \parallel \\ j \end{smallmatrix} \right\}_N^6 \left\{ \begin{smallmatrix} l \\ \parallel \\ k \end{smallmatrix} \right\}_N^3 \left\{ \begin{smallmatrix} l \\ \parallel \\ i \end{smallmatrix} \right\}_N^4} \right\} \quad (3.1)$$

where N is the total number of lattice points in the system. This entropy expression is known to be the most efficient one when the tetrahedron is used as the variable^{7,8,10,11} for bcc. The powers in (3.1) are derived from the procedure of correcting over-counting as mentioned in section 1. The curly bracket notation is the standard one used in the CVM^{7,8,10,11} and is, for example,

$$\{i\}_N \equiv \prod_i (Nx_i)^{i^i} \quad (3.2)$$

Using Stirlings approximation, we can write (3.1) explicitly as

$$S/kN = -6 \sum_{i=1}^{10} g_i \mathcal{L}(w_i) + 12 \sum_{i=1}^8 g_i^{(u)} \mathcal{L}(u_i) \quad (3.3)$$

$$- 3 \sum_{i=1}^3 g_i^{(z)} \mathcal{L}(z_i) - 4 \sum_{i=1}^4 g_i^{(y)} \mathcal{L}(y_i) + \sum_{i=1}^2 g_i^{(x)} \mathcal{L}(x_i).$$

where $\mathcal{L}(x)$ is short for $\mathcal{L}(x) \equiv x \ln x - x$, and where the variables u , z , y , and x are to be expressed in the variable w . We would like to point out that in Bell's calculation¹ the term in w and the term in x were included but that the terms in u , z , and y were omitted. Our expression (3.3) is known^{12,13} to give more reliable results than the one used by Bell. We first make the formulation symmetric; for instance we write:

$$3 \mathcal{L}(z_{ij}) = 3/2 (\mathcal{L}(z_{ij}) + \mathcal{L}(z_{kl})) \quad (3.4)$$

and then compute the derivative which can be written in general as:

$$\begin{aligned} \frac{dS}{dw_i} / kN = & -6 \ln w_i + 3 \sum_{j=1}^8 D_{ij} \ln u_j - \\ & - \frac{3}{2} \sum_{j=9}^{11} D_{ij} \ln z_{j-8} - \sum_{j=12}^{15} D_{ij} \ln y_{j-12} \\ & + \frac{1}{4} \sum_{j=16}^{17} D_{ij} \ln x_{j-16} \quad (i=1, \dots, 10) \end{aligned} \quad (3.5)$$

where D_{ij} are the elements of the decomposition matrix (D-matrix) which is to be explained in (3.6) below.

Let us make a short remark about the new labels: the subscripts "ijkl" represent $2^4 = 16$ options. In a non-hydrogen bonded model they can be replaced by five options with appropriate weight factors g_t . In Fig. 2 they have to be

replaced by ten options to distinguish between the possible presences and absences of the hydrogen bonds. We think the figure speaks for itself.

The elements of the decomposition matrix can be written down immediately by considering the number of ways a tetrahedral cluster can be broken up into its constituent elements; that is, into triangles, double bonded pairs, single bonded pairs, and sites. We found a simple relation between the elements of the CR-matrix and the elements of the D-matrix:

$$D_{ij} = \frac{f_i g_i}{g_j} C_{ij} \quad (3.6)$$

where f_1 equals four, except for the parameters z , where $f_1 = 2$. This relation also has the practical value that it simplifies the data input in the computation.

The breakdown of the tetrahedrons into subclusters is not entirely unambiguous. The point variables x_2 represent an occupied site. The molecule on such an occupied site can be oriented in two different sets of 6 directions and this will determine how the diagram has to be completed into a y-pair. Each completion can lead to a different linear combination of pair-clusters using y_3 or y_4 and there is no a priori guarantee that these two equations give the same result for the variable x_2 . The correct way to assure this is to introduce a separate Lagrange multiplier, which leads to a minor iteration in the natural iteration method.¹¹ An alternate way is simply to take

the average, in this case one to seven. We computed both cases and found not much difference in the final result for the order parameters of the 10 tetrahedrons, at least not in the region of temperatures and chemical potential used. The issue was not further pursued because in the extended model³ the two orientations of the molecule on a given site were explicitly introduced in the model and consequently this bifurcation does not occur.

To construct G/N , the grand potential per lattice site, we have to add two more terms to the expression for TS. One represents the energy of the various occupations of the cluster and one term contains the chemical potential; in total:

$$6 \sum (\xi_i - a_i \mu / 24) g_i w_i \quad (3.7)$$

Where a_i is the number of occupied sites in the cluster w_i , i.e. the number of black circles in w_i of Fig. 2. The expression for the energies ξ_i are written as linear combinations of the three basic parameters: ξ_p the pair energy in the absence of a hydrogen bond, ξ_H the additional pair energy in the presence of a hydrogen bond and ξ_{nnn} the next nearest neighbor repulsion. The numerical factors stem from the fact that there are 6 tetrahedrons per lattice site, containing a total of 24 sites.

Finally we add a Lagrange multiplier term, of the form:

$$\lambda (1 - \sum_{i=1}^{10} g_i w_i) \quad (3.8)$$

in order to maintain the normalization condition.

Combining these relations, the grand potential G is written as

$$\begin{aligned} \Phi \equiv \beta G/N = & 6\beta \sum_{i=1}^{10} \left(\varepsilon_i - \frac{\nu}{24} a_i \right) g_i w_i + 6 \sum_{i=1}^{10} g_i \mathcal{L}(w_i) \\ & - 12 \sum_{i=1}^8 g_i^{(u)} \mathcal{L}(u_i) + 3 \sum_{i=1}^3 g_i^{(z)} \mathcal{L}(z_i) + 4 \sum_{i=1}^4 g_i^{(y)} \mathcal{L}(y_i) \quad (3.9) \\ & - \sum_{i=1}^2 g_i^{(x)} \mathcal{L}(x_i) - \lambda \beta \left[1 - \sum_{i=1}^{10} g_i w_i \right] \end{aligned}$$

When this is minimized with respect to w_1 , we obtain, for example,

$$\begin{aligned} \frac{\partial \Phi}{\partial w_4} = & 74 \left[6\beta \left(\varepsilon_4 - \frac{\nu}{24} a_4 \right) + 6 \ln w_4 - 3 \ln(u_2 u_2 u_6 u_6) \right. \\ & + (3/2) \ln(z_2 z_2) + \ln(y_1 y_2 y_2 y_4) \quad (3.10) \\ & \left. - (\frac{1}{4}) \ln(x_1 x_1 x_2 x_2) - \beta \lambda \right] = 0 \end{aligned}$$

This expression has an easily understandable physical meaning. When we look at w_4 in Fig. 2, we see that it contains $2u_2$'s, $2u_6$'s, $2z_2$'s, y_1 , $2y_2$'s, y_4 , $2x_1$'s and $2x_2$'s. These subclusters appear in the equation. The coefficients on logarithm terms originate in Eq.(3.9). All of the derivatives

$\partial\Phi/\partial w_i$ ($i = 1, \dots, 10$), which are derived from Eq.(3.9), can be interpreted in the same way.

When these derivatives vanish, we can see the meaning of by forming

$$\bar{\Phi} = \Phi - \sum_{i=1}^{10} w_i \frac{\partial\Phi}{\partial w_i} = \beta\lambda = \beta \frac{G}{N} \quad (3.11)$$

Hence the Lagrange multiplier λ is equal to G/N when the iteration has converged.

From the grand potential we find immediately the pressure p , since it is given by

$$\lambda = \frac{G}{N} = -p \frac{V}{N} = -p \frac{a^3}{2} \quad (3.12)$$

where a is the length of the edge of the bcc cube. In order to determine the equation of state we need to know the density ρ . This quantity can be either expressed in terms of the a_i 's that are used in the chemical potential term as :

$$\rho = \sum_{i=2}^{10} a_i g_i w_i \equiv \langle a \rangle \quad (3.13a)$$

or directly by using:

$$\rho = 12 X_2 \quad (3.1;3b)$$

the relation between these two expressions can be obtained by

writing x_2 in terms of the order parameters w_i as given by the column of the CR-matrix. We find

$$x_2 = 4 \sum_{i=2}^{10} C(i, 27) w_i / g_i \quad (3.14)$$

Next we can compute the two additional observable quantities: the number of nearest neighbor pairs, $18 (7y_3 + y_4)$ and the number of next nearest neighbor pairs, $144 z_3$. These quantities have been reported in X-ray experiments and have the fascinating property that they remain rather "ice-like" in the low temperature region of the liquid.¹⁴

Finally we report a similar, but not directly observable, quantity: the relative number of hydrogen bonded nearest neighbor pairs:

$$R_H = \frac{y_4}{7y_3 + y_4} \quad (3.15)$$

Although this model cannot give the angular correlation between two neighboring molecules, R_H is in a certain way a measure of this angular correlation. The latter can be experimentally extracted from the results of polarized light scattering experiments.

4. Choice of Energy Parameters.

The model we used contains four adjustable parameters. One more, the lattice constant, is needed in case the grand partition function is converted into a pressure. These four parameters are:

1. the nearest neighbor attractive interaction in the absence of the hydrogen bond,
2. the additional attractive energy introduced when the relative orientation between a pair of molecules leads to a hydrogen bond,
3. a repulsive energy that discourages the simultaneous occupation of next nearest neighbor sites. This can be introduced in the form of a repulsive three body force or through two body (next-nearest neighbor) repulsive force. The latter seems to us more realistic.

It has been suggested that there may be a three body force detectable in the vapor phase of water and other gases. Direct evidence for such a force is hard to come by. Very often the three body force was inserted in the calculations of the virial coefficients to make up for discrepancies between the computation and the experiment. The presence of open ice suggests that in a certain range of temperatures and pressures, the occupation of next-nearest neighbors is discouraged. (We can justify this in a schematic way by proving that the number of relative orientations with repulsive energy exceeds the number of pair orientations

with attractive energy for next-nearest neighbor sites; see Appendix II.) This can be accomplished in the model by introducing either a next-nearest neighbor repulsive force or by a repulsive three body force.

As to the most realistic values for the interaction constants, even if the interaction between water molecules were precisely known,^{15,16,17} it is hard to assess how potential energy functions would have to be translated into the parameters of such a schematic model. Roughly speaking the interaction energy ϵ_p is about 1.5 kcal/mol (corresponds to $\epsilon_p/k = 700K$). To estimate the H-bond potential we use the probability of broken H-bonds as introduced by Luck and Ditter¹⁶. Their result for this probability $P(T)$ can be represented by

$$P(T) \sim \exp(2200/T)$$

which leads to $\epsilon_H/k = -500$ for the H-bond potential. Although these values should not be taken too seriously, it is interesting to notice that they lead to a critical temperature (and critical pressure) that lies in the neighborhood of the observed values.

The next-nearest neighbor repulsion is very difficult to assess. Hence we are only guided by the need that its value must lie above $(2/3)\epsilon_{nn}$ in order to obtain open ice at low pressure values.

5. Results

The computations were executed for a number of potentials. We report here only one or two cases, since it became clear that this simple model always lacks details at high densities since the average over two orientations were taken. The main search was to see whether we could reproduce the density maximum that was found in the molecular field model. The potential that showed the desired features most clearly is given by $\Sigma_p = 1000$, $\Sigma_H = 2500$, and $\Sigma_{HH} = 500$ K. See Figure 3. The isotherms are given for five different temperatures: $T = 300, 325, 350, 375$ and 400 K. The points were obtained by lowering the absolute value of μ , the chemical potential. μ is negative. In each new point the values of w 's of the preceding point are used as initial conditions for the iteration. Each isotherm starts at a high density-high pressure point and then comes down in pressure. At a certain value of the chemical potential, and corresponding pressure, the number of iterations increases and the calculation becomes susceptible to a transition to a different value of the density. In this particular calculation this happens twice, except for the high temperature isotherm which is smoothly going from high density to low density. It can be seen from the chemical potential versus ρ at low temperatures, that for the given potential there are two different slopes, one between 0 and $1/2$ and a different one between $1/2$ and 1, consequently there are two transitions: one from the low density or gas phase to the one-half density or open ice phase and one from that phase to the high density or liquid phase.

The center part of the plot shows that the isotherms are crossing each other. This implies that there is a density maximum, since the density is the same at two different temperatures. This is plotted separately in Figure 4. The dotted line indicates the phase transition.

Appendix I

Cluster relation (CR) matrix.

This matrix represents the value of each subcluster as expressed in a linear combination of the principal clusters. The 10 principal clusters are the possible occupations of the four sites of the tetrahedron with and without hydrogen bonds. Although this information can be deduced from the text, we repeat it here so that we can use it in future extensions of the model. The matrix C is related to the decomposition matrix D in a simple manner, see (3.6). We used this relation to check the matrix elements of C. The results are given in Table I.

Appendix II

Next nearest neighbor repulsion.

Since the next-nearest neighbor repulsion seems to be an essential part of the model, we give the following suggestion. Suppose we deal with 3 molecules, as shown in Fig. A1; each molecule has a dipole moment, and takes 12 orientations dictated by the model. Then the dipole moment $\vec{\mu}$ will be oriented (twice) in the $\pm x$, $\pm y$, and $\pm z$ directions, and the dipolar coupling energy between 1 and 2 and between 2 and 3 is given by:

$$\mathcal{H}_{12} = -E (\mu_1^x \mu_2^y + \mu_1^y \mu_2^x + \mu_1^z \mu_2^z);$$

$$\mathcal{H}_{23} = -E (\mu_2^x \mu_3^y - \mu_2^y \mu_3^x - \mu_2^z \mu_3^z),$$

using the dipolar tensor. If we consider the six possible directions of $\vec{\mu}_1$, we find that the lowest energy is obtained for 24 different arrangements. If we now consider the relative orientations of dipole 1 with respect to dipole 3 we find that 16 have zero energy, 4 have energies that mutually cancel out and 4 are repulsive. These 4 are antiparallel along the z axis.

We may repeat this combinatorial exercise assuring the presence of an H-bond between either 1 and 2 or 2 and 3 and we find again that the relative orientations between 2 and 3 in which the dipolar interaction is repulsive are favored. Since this reasoning depended on the presence of an intermediary

molecule, this model seems to favor the concept of an effective three body force.

List of Figures

1. Insertion of the tetrahedron in the bcc lattice and its subdivision in two diamond lattices.
2. Tetrahedrons with and without hydrogen bonding, and the resulting subclusters required to obtain the Kikuchi entropy expression.
3. Isotherms for $T = 300, 325, 350, 375$ and 400 K using the potential given by $\epsilon_p = -1300$, $\epsilon_H = 2500$ and $\epsilon_{nnn} = 300$ K. The crossing of the isotherms means a density maximum.
4. Direct computation of the density maximum for the same potential .
5. (A1). Positioning of three molecules: 1-2 and 2-3 are nearest neighbors and 1-3 are next-nearest neighbors.

REFERENCES

1. G. M. Bell, J. Phys. C Sol. State Phys. 5, 889, 1972.
2. G. M. Bell and D. W. Salt, Farad. Trans. II, 72, 76, 1976.
3. See following article.
4. A. H. Narten, M. D. Danford and H. A. Levy, Discussions Faraday Soc. 43, 97, 1967.
5. F. H. Stillinger, Adv. Chem. Phys. (Prigogine and Rice, eds.) 31, 1, 1975. John Wiley and Son.
6. P. D. Flemming and J. H. Gibbs, J. Stat. Phys. 10, 157 and 351, 1974.
7. J. Heilmann and D. A. Huckaby, J. Stat. Phys. 20, 371, 1979.
8. W.A.R. Luck and W. Ditter, J. [Chem.] Phys. 74, 3687, 1970.
9. L. Pauling, J. Am. Chem. Soc. 57, 2680, 1935.
10. D. Eisenberg and W. Kauzmann, The Structure and Properties of Water, Oxford, Clarendon, 1969.
11. R. Kikuchi, Phys. Rev. 81, 988, 1951.
12. R. Kikuchi and C. M. van Baal, Scripta Metallurgica 8, 425, 1974.
13. R. Kikuchi and H. Sato, Acta Metallurgica 22, 1099, 1974.
14. T. Morita, J. Phys. Soc. Jpn. 12, 753, 1060, 1957.
15. R. Kikuchi, J. Chem. Phys. 60, 1071, 1974.
16. R. Kikuchi, J. Chem. Phys. 65, 4545, 1976.
17. J. A. Barker, Proc. Roy. Soc. A216, 45, 1953.
18. E. A. Guggenheim and M. L. McGlashen, Molecular Physics 5, 433, 1962.

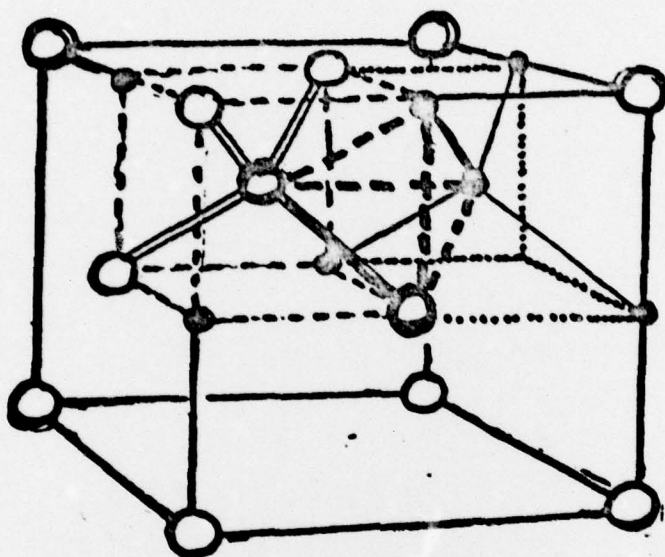


FIG 1.

ε_n	w	$g_t(g_0)$	subclusters:		
			u	weight	
$\varepsilon_1 = 0$		1		1	
$\varepsilon_2 = 0$		4(12)		2(12)	
$\varepsilon_3 = -\varepsilon_{nnn}$		2(12^2)		12	
		4(18)		12^2	
$\varepsilon_4 = -\varepsilon_p - \varepsilon_H$		4(18)		2(7.18)	
$\varepsilon_5 = -\varepsilon_p$		4(7.18)		2(18)	
		4(7.18)		72.18	
$\varepsilon_6 = -2\varepsilon_p - \varepsilon_H + \varepsilon_{nnn}$		8(12.18)		2(12.18)	
$\varepsilon_7 = -2\varepsilon_p + \varepsilon_{nnn}$		4(72.18)			
$\varepsilon_8 = \varepsilon_{10} - 2\varepsilon_H$		2(18^2)	\mathcal{Z}		1
$\varepsilon_9 = \varepsilon_{10} - \varepsilon_H$		4(7.18^2)			2(12)
$\varepsilon_{10} = -4\varepsilon_p + 2\varepsilon_{nnn}$		(34.18)			(12^2)
			\mathcal{Y}		1
					12
					(7.18)
					(18)
			\mathcal{X}		1
					12

FIG. 2

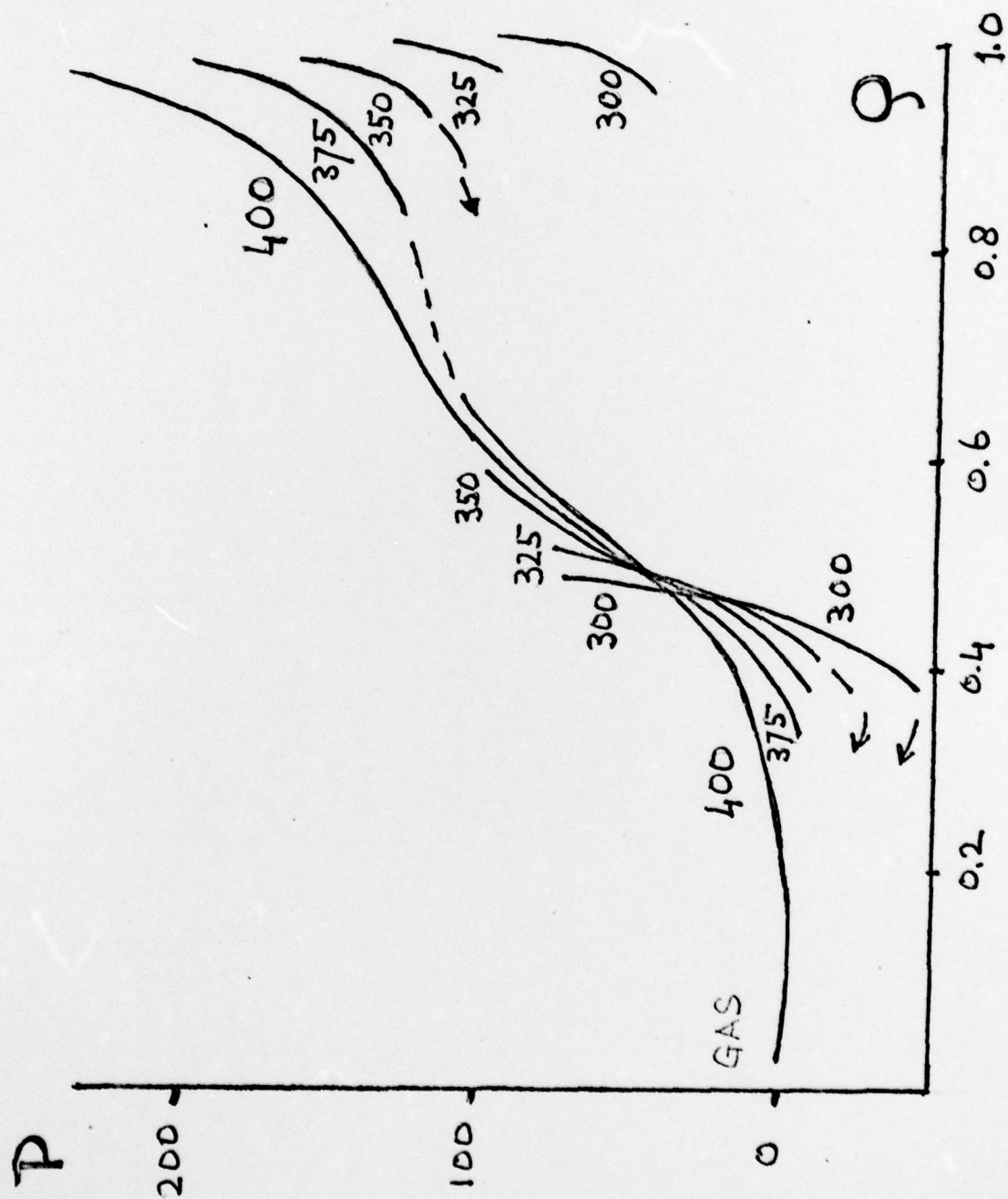


Fig 2

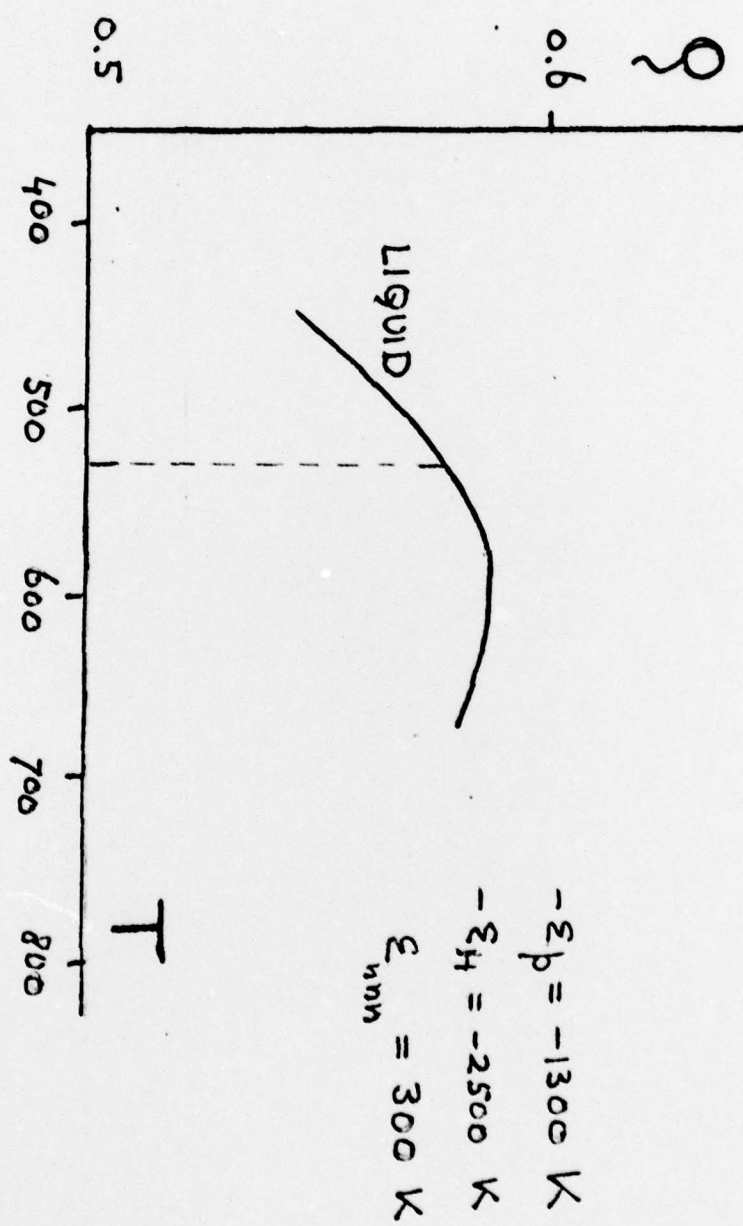


FIG 4

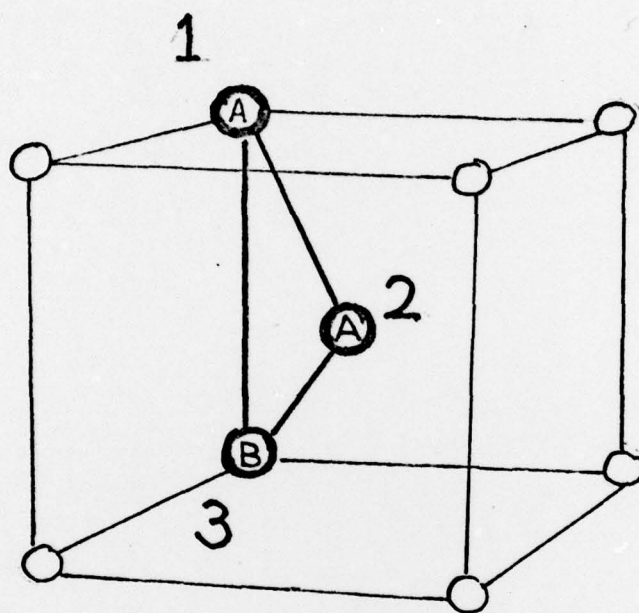


FIG A1

Cluster Relations with H-bond

	Weight factors		1	2	3	4	5	6	7	8	9	10
U1	1	1	1	12								
U2	2	12		1		3/2	21/2					
U3	1	12		1	12							
U4	1	(12) ²			1			3	9			
U5	2	7.18					1	(12/7)	(72/7)			
U6	2	18				1		12				
U7	1	12.6.18							1		7/2	17/2
U8	2	18.12						1		3/2	21/2	
Z1	1	1	1	24	144	0	0	0	0	0	0	0
Z2	2	12	0	1	0	3	21	36	108	0	0	0
Z3	1	(12) ²	0	0	1	0	0	6	18	9/2	63	153/2
Y1	1	1	1	24	0	18	126	0	0	0	0	0
Y2	2	12	0	1	12	3/2	21/2	36	108	0	0	0
Y3	1	7.18	0	0	0	0	1	(24/7)	(144/7)	(18/7)	54	(612/7)
Y4	1	18	0	0	0	1	0	24	0	18	126	0
X1	1	1	1	36	144	36	252	432	1296	0	0	0
X2	1	12	0	1	12	3	21	108	324	54	756	918

TABLE I

TECHNICAL REPORT DISTRIBUTION LIST, GEN

	<u>No. Copies</u>		<u>No. Copies</u>
Office of Naval Research 800 North Quincy Street Arlington, Virginia 22217 Attn: Code 472	2	Defense Documentation Center Building 5, Cameron Station Alexandria, Virginia 22314	12
ONR Branch Office 536 S. Clark Street Chicago, Illinois 60605 Attn: Dr. George Sandoz	1	U.S. Army Research Office P.O. Box 1211 Research Triangle Park, N.C. 27709 Attn: CRD-AA-IP	1
ONR Branch Office 715 Broadway New York, New York 10003 Attn: Scientific Dept.	1	Naval Ocean Systems Center San Diego, California 92152 Attn: Mr. Joe McCartney	1
ONR Branch Office 1030 East Green Street Pasadena, California 91106 Attn: Dr. R. J. Marcus	1	Naval Weapons Center China Lake, California 93555 Attn: Dr. A. B. Amster Chemistry Division	1
ONR Area Office One Hallidie Plaza, Suite 601 San Francisco, California 94102 Attn: Dr. P. A. Miller	1	Naval Civil Engineering Laboratory Port Hueneme, California 93401 Attn: Dr. R. W. Drisko	1
ONR Branch Office Building 114, Section D 666 Summer Street Boston, Massachusetts 02210 Attn: Dr. L. H. Peebles	1	Professor K. E. Woehler Department of Physics & Chemistry Naval Postgraduate School Monterey, California 93940	1
Director, Naval Research Laboratory Washington, D.C. 20390 Attn: Code 6100	1	Dr. A. L. Slafkosky Scientific Advisor Commandant of the Marine Corps (Code RD-1) Washington, D.C. 20380	1
The Assistant Secretary of the Navy (R,E&S) Department of the Navy Room 4E736, Pentagon Washington, D.C. 20350	1	Office of Naval Research 800 N. Quincy Street Arlington, Virginia 22217 Attn: Dr. Richard S. Miller	1
Commander, Naval Air Systems Command Department of the Navy Washington, D.C. 20360 Attn: Code 310C (H. Rosenwasser)	1	Naval Ship Research and Development Center Annapolis, Maryland 21401 Attn: Dr. G. Bosmajian Applied Chemistry Division	1
		Naval Ocean Systems Center San Diego, California 91232 Attn: Dr. S. Yamamoto, Marine Sciences Division	1

TECHNICAL REPORT DISTRIBUTION LIST, 051B

	<u>No.</u> <u>Copies</u>		<u>No.</u> <u>Copies</u>
Professor K. Wilson University of California, San Diego Department of Chemistry, B-014 La Jolla, California 92093	1	Dr. B. Vonnegut State University of New York Earth Sciences Building 1400 Washington Avenue Albany, New York 12203	1
Professor C. A. Angell Purdue University Department of Chemistry West Lafayette, Indiana 47907	1	Dr. Hank Loos Laguna Research Laboratory 21421 Stans Lane Laguna Beach, California 92651	1
Professor P. Meijer Catholic University of America Department of Physics Washington, D.C. 20064	1	Dr. John Latham University of Manchester Institute of Science & Technology P.O. Box 88 Manchester, England M60 1QD	1
Dr. S. Greer Chemistry Department University of Maryland College Park, Maryland 20742	1	Professor P. Delahay New York University 100 Washington Square East New York, New York 10003	1
Dr. T. Ashworth South Dakota School of Mines & Technology Department of Physics Rapid City, South Dakota 57701	1		
Dr. G. Gross New Mexico Institute of Mining & Technology Socorro, New Mexico 87801	1		
Dr. J. Kassner University of Missouri - Rolla Space Science Research Center Rolla, Missouri 65401	1		
Dr. J. Telford University of Nevada System Desert Research Institute Lab of Atmospheric Physics Reno, Nevada 89507	1		